Meccanica **38:** 467–475, 2003.
© 2003 *Kluwer Academic Publishers. Printed in the Netherlands.*

BRIEF NOTE

Two Collinear Permeable Cracks in a Piezoelectric Layer Bonded to Two Half Spaces

ZHEN-GONG ZHOU, JUN LIANG and BIAO WANG
Center for Composite Materials and Electro-Optics Research Center, Harbin Institute of Technology, P.O. Box 1247, Harbin 150001, P.R. China

(Received: 5 September 2001; accepted in revised form: 16 February 2002)

Key words: Collinear cracks, Piezoelectric materials, Schmidt method, Fourier transform.

1. Introduction

In the theoretical studies of crack problems in piezoelectric materials, several different electric boundary conditions at the crack surfaces have been proposed by numerous researchers. For example, for the sake of analytical simplification, the assumption that the crack surfaces are impermeable to electric fields was adopted by many researchers [1–3]. In this model, the assumption of the impermeable cracks refers to the fact that the crack surfaces are free of surface charge and thus the electric displacement vanishes inside the crack. In fact, cracks in piezoelectric materials consist of vacuum, air or some other gas. This requires that the electric fields can propagate through the crack, so the electric displacement component perpendicular to the crack surfaces should be continuous across the crack surfaces [4]. It is interesting to note that very different results were obtained by changing the boundary conditions [5]. In the present paper, the interaction between two collinear symmetrical permeable cracks subject to anti-plane shear in piezoelectric layer bonded to two half spaces is investigated by use of the Schmidt method [6]. The cracks are situated symmetrically and oriented in the direction vertically to the interfaces of the layer. This is quite different from that in [3].

2. Formulation of the Problem

Consider a piezoelectric layer that is sandwiched between two elastic half planes with an elastic stiffness constant c_{44}^{E}. Quantities in the half spaces will subsequently be designated by superscript E. The piezoelectric material layer of thickness $2h$ contains two cracks of length $1 - b$ that are vertical to the interfaces, as shown in Figure 1. $2b$ is the distance between the cracks. (The solution of two collinear Griffith cracks of length $a - b$ can easily be obtained by a simple change in the numerical values of the present paper. $a > b > 0$.) As discussed in [5], permeable condition will be enforced in the present study. So the boundary conditions of the present problem are

$$\begin{aligned} &w^{(1)} = w^{(2)}, \qquad \tau_{yz}^{(1)} = \tau_{yz}^{(2)}, \qquad \phi^{(1)} = \phi^{(2)}, \qquad D_y^{(1)} = D_y^{(2)}, \\ &y = 0, \ \ |x| \leqslant b, \quad 1 \leqslant |x| \leqslant h \end{aligned} \tag{1}$$

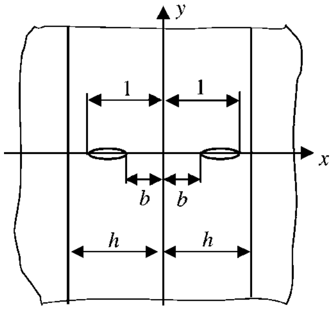

Figure 1. Cracks in a piezoelectric layer body under anti-plane shear.

$$\tau_{yz}^{(1)} = \tau_{yz}^{(2)} = -\tau_0, \qquad \phi^{(1)} = \phi^{(2)}, \qquad D_y^{(1)} = D_y^{(2)}, \quad y = 0, \ b \leqslant |x| \leqslant 1 \tag{2}$$

$$\begin{aligned} &\tau_{xz}^{(1,2)}(\pm h, y) = \tau_{xz}^{\mathrm{E}}(\pm h, y), \qquad w^{(1,2)}(\pm h, y) = w^{\mathrm{E}}(\pm h, y), \\ &D_x^{(1,2)}(\pm h, y) = 0 \end{aligned} \tag{3}$$

$$w^{(1)} = w^{(2)} = w^{\mathrm{E}} = 0 \quad \text{for } (x^2 + y^2)^{1/2} \to \infty \tag{4}$$

where $\tau_{zk}^{(1,2)}$ and $D_k^{(1,2)}$ $(k = x, y)$ are the anti-plane shear stress and in-plane electric displacement, respectively. $w^{(1,2)}$ and $\phi^{(1,2)}$ are the mechanical displacement and electric potential. τ_{xz}^{E}, τ_{yz}^{E} and w^{E} are the shear stress, and the displacement in the half elastic spaces, respectively. Note that all quantities with superscript k $(k = 1, 2)$ refer to the upper plane $(y \geqslant 0)$ and the lower plane $(y \leqslant 0)$ as in Figure 1, respectively.

The constitutive equation can be written as

$$\begin{aligned} &\tau_{zk}^{(1,2)} = c_{44} w_{,k}^{(1,2)} + e_{15}\phi_{,k}^{(1,2)}, \qquad D_k^{(1,2)} = e_{15} w_{,k}^{(1,2)} - \varepsilon_{11}\phi_{,k}^{(1,2)}, \\ &\tau_{kz}^{\mathrm{E}} = c_{44}^{\mathrm{E}} w_{,k}^{\mathrm{E}} \quad (k = x, y) \end{aligned} \tag{5}$$

where c_{44}, e_{15} and ε_{11} are the shear modulus, piezoelectric coefficient and dielectric parameter, respectively. The anti-plane governing equations are

$$\begin{aligned} &c_{44}\nabla^2 w^{(1,2)} + e_{15}\nabla^2\phi^{(1,2)} = 0, \qquad e_{15}\nabla^2 w^{(1,2)} - \varepsilon_{11}\nabla^2\phi^{(1,2)} = 0, \\ &\nabla^2 w^{\mathrm{E}} = 0 \end{aligned} \tag{6}$$

where $\nabla^2 = \partial^2/\partial x^2 + \partial^2/\partial y^2$ is the two-dimensional Laplace operator. Because of the assumed symmetry in geometry and loading, it is sufficient to consider the problem for $0 \leqslant x < \infty$, $-\infty < y < \infty$ only. The solutions of (6) can be assumed as

$$\begin{aligned} w^{(1)}(x, y) \ = \ &\frac{2}{\pi}\int_0^\infty A_1(s)\,\mathrm{e}^{-sy}\cos(sx)\,\mathrm{d}s \\ &+ \frac{2}{\pi}\int_0^\infty H(s)\cosh(sx)\sin(sy)\,\mathrm{d}s \quad (y \geqslant 0) \end{aligned} \tag{7}$$

$$w^{(2)}(x,y) = \frac{2}{\pi}\int_0^\infty A_2(s)\,\mathrm{e}^{sy}\cos(sx)\,\mathrm{d}s + \frac{2}{\pi}\int_0^\infty H(s)\cosh(sx)\sin(sy)\,\mathrm{d}s \quad (y \leqslant 0) \tag{8}$$

$$w^{\mathrm{E}}(x,y) = \frac{2}{\pi}\int_0^\infty C(s)\,\mathrm{e}^{-sx}\sin(sy)\,\mathrm{d}s \tag{9}$$

where $A_1(s)$, $A_2(s)$, $H(s)$ and $C(s)$ are unknown functions. Inserting (7) and (8) into (6), it can be assumed

$$\phi^{(1)}(x,y) - \frac{e_{15}}{\varepsilon_{11}}w^{(1)}(x,y) = \frac{2}{\pi}\int_0^\infty B_1(s)\,\mathrm{e}^{-sy}\cos(sx)\,\mathrm{d}s + \frac{2}{\pi}\int_0^\infty F(s)\cosh(sx)\sin(sy)\,\mathrm{d}s \tag{10}$$

$$\phi^{(2)}(x,y) - \frac{e_{15}}{\varepsilon_{11}}w^{(2)}(x,y) = \frac{2}{\pi}\int_0^\infty B_2(s)\,\mathrm{e}^{sy}\cos(sx)\,\mathrm{d}s + \frac{2}{\pi}\int_0^\infty F(s)\cosh(sx)\sin(sy)\,\mathrm{d}s \tag{11}$$

where $B_1(s)$, $B_2(s)$ and $F(s)$ are unknown functions.

So from (5), the following can be given:

$$\begin{aligned}
\tau_{yz}^{(1)}(x,y) &= -\frac{2}{\pi}\int_0^\infty s\big\{[\mu A_1(s) + e_{15}B_1(s)]\,\mathrm{e}^{-sy}\cos(sx) \\
&\quad - [\mu H(s) + e_{15}F(s)]\cos(sy)\cosh(sx)\big\}\,\mathrm{d}s \\
D_y^{(1)}(x,y) &= \frac{2}{\pi}\int_0^\infty \varepsilon_{11}s[B_1(s)\,\mathrm{e}^{-sy}\cos(sx) \\
&\quad - F(s)\cos(sy)\cosh(sx)]\,\mathrm{d}s \quad (y \geqslant 0)
\end{aligned} \tag{12}$$

$$\begin{aligned}
\tau_{yz}^{(2)}(x,y) &= \frac{2}{\pi}\int_0^\infty s\big\{[\mu A_2(s) + e_{15}B_2(s)]\,\mathrm{e}^{sy}\cos(sx) \\
&\quad + [\mu H(s) + e_{15}F(s)]\cos(sy)\cosh(sx)\big\}\,\mathrm{d}s \\
D_y^{(2)}(x,y) &= -\frac{2}{\pi}\int_0^\infty \varepsilon_{11}s[B_2(s)\,\mathrm{e}^{sy}\cos(sx) \\
&\quad + F(s)\cos(sy)\cosh(sx)]\,\mathrm{d}s \quad (y \leqslant 0)
\end{aligned} \tag{13}$$

$$\tau_{xz}^{\mathrm{E}}(x,y) = -\frac{2}{\pi}\int_0^\infty c_{44}^{\mathrm{E}}sC(s)\,\mathrm{e}^{-sx}\sin(sy)\,\mathrm{d}s, \qquad \mu = c_{44} + \frac{e_{15}^2}{\varepsilon_{11}} \tag{14}$$

To solve the problem, the gap functions of the crack surface displacements and the electric potentials are defined as follows:

$$f(x) = w^{(1)}(x, 0^+) - w^{(2)}(x, 0^-), \qquad f_\phi(x) = \phi^{(1)}(x, 0^-) - \phi^{(2)}(x, 0^-) \tag{15}$$

Substituting (7)–(11) into (15), and applying the Fourier transform and the boundary conditions, the following can be obtained:

$$\bar{f}(s) = A_1(s) - A_2(s), \qquad \bar{f}_\phi(s) = \frac{e_{15}}{\varepsilon_{11}}\bar{f}(s) + B_1(s) - B_2(s) = 0 \tag{16}$$

$$\mu[A_1(s) + A_2(s)] + e_{15}[B_1(s) + B_2(s)] = 0, \quad B_1(s) + B_2(s) = 0 \tag{17}$$

By solving four equations (16) and (17) with four unknown functions $A_1(s)$, $A_2(s)$, $B_1(s)$, $B_2(s)$ and applying the boundary conditions (2), the following can be obtained:

$$\int_0^\infty s\big\{c_{44}\bar{f}(s)\cos(sx) - [\mu H(s) + e_{15}F(s)]\cosh(sx)\big\}\,\mathrm{d}s = \pi\tau_0, \quad b \leqslant |x| \leqslant 1 \tag{18}$$

$$\int_0^\infty \bar{f}(s)\cos(sx)\,\mathrm{d}s = 0, \quad |x| > 1 \text{ and } |x| < b \tag{19}$$

The relationships between the functions $A_1(s)$, $A_2(s)$, $B_1(s)$, $B_2(s)$, $F(s)$, $H(s)$ and $C(s)$ are obtained by applying a Fourier sine transform to equation (3):

$$H(t)[\sinh(th) + \mu_1\cosh(th)] = \frac{2}{\pi}\int_0^\infty \frac{\sin(sh)s - t\mu_1\cos(sh)}{s^2 + t^2}A_1(s)\,\mathrm{d}s \tag{20}$$

$$C(t)\,\mathrm{e}^{-th}[\sinh(th) + \mu_1\cosh(th)] = \frac{2}{\pi}\int_0^\infty \frac{\cosh(th)\sin(sh)s + \sinh(th)\cos(sh)t}{s^2 + t^2}A_1(s)\,\mathrm{d}s \tag{21}$$

$$F(t)\sinh(th) = \frac{2}{\pi}\int_0^\infty \frac{s}{s^2 + t^2}B_1(s)\sin(sh)\,\mathrm{d}s, \quad \mu_1 = \frac{c_{44}^{\mathrm{E}}}{\mu} \tag{22}$$

3. Solution of the Triple Integral Equation

To solve the problem, the gap functions of the crack surface displacement are represented by the following series:

$$f(x) = \sum_{n=0}^{\infty} a_n P_n^{(1/2,1/2)}\left(\frac{x - (1+b)/2}{(1-b)/2}\right)\left(1 - \frac{(x - (1+b)/2)^2}{((1-b)/2)^2}\right)^{1/2} \quad \text{for } b \leqslant |x| \leqslant 1, \quad y = 0 \tag{23}$$

where a_n are the unknown coefficients to be determined and $P_n^{(1/2,1/2)}(x)$ is a Jacobi polynomial [7]. The Fourier transformation of equation (23) is

$$\bar{f}(s) = \sum_{n=0}^{\infty} a_n Q_n G_n(s) \frac{1}{s} J_{n+1}\left(s\frac{1-b}{2}\right) \tag{24}$$

$$Q_n = 2\sqrt{\pi}\frac{\Gamma(n+1+1/2)}{n!},$$
$$G_n(s) = \begin{cases} (-1)^{n/2}\cos\left(s\dfrac{1+b}{2}\right), & n = 0, 2, 4, 6, \dots \\ (-1)^{(n+1)/2}\sin\left(s\dfrac{1+b}{2}\right), & n = 1, 3, 5, 7, \dots \end{cases} \tag{25}$$

where $\Gamma(x)$ and $J_n(x)$ are the Gamma and Bessel functions, respectively.

Substituting (24) into (18) and (19), respectively, equations (19) can be automatically satisfied. Then the remaining equation (18) reduces to the form after integration with respect to x in $[b, x]$.

$$\begin{aligned} &c_{44}\sum_{n=0}^{\infty} a_n Q_n \int_0^{\infty} s^{-1} G_n(s) J_{n+1}\left(s\frac{1-b}{2}\right)[\sin(sx) - \sin(sb)]\,\mathrm{d}s = \pi\tau_0(x-b) \\ &\quad + \frac{\mu}{\pi}\sum_{n=0}^{\infty} a_n Q_n \int_0^{\infty} \frac{\sinh(sx) - \sinh(sb)}{\sinh(sh) + \mu_1\cosh(sh)}\,\mathrm{d}s \\ &\qquad \int_0^{\infty} G_n(\eta) J_{n+1}\left(\eta\frac{1-b}{2}\right)\frac{\eta\sin(\eta h) - s\mu_1\cos(\eta h)}{(\eta^2+s^2)\eta}\,\mathrm{d}\eta \\ &\quad - \frac{e_{15}^2}{\pi\varepsilon_{11}}\sum_{n=0}^{\infty} a_n Q_n \int_0^{\infty} \frac{\sinh(sx) - \sinh(sb)}{\sinh(sh)}\,\mathrm{d}s \\ &\qquad \int_0^{\infty} G_n(\eta) J_{n+1}\left(\eta\frac{1-b}{2}\right)\frac{\sin(\eta h)}{\eta^2+s^2}\,\mathrm{d}\eta \end{aligned} \tag{26}$$

For a large s, the integrands of the double semi-infinite integral in equation (26) almost all have exponential forms, so the double semi-infinite integral can be evaluated numerically. Equation (26) can now be solved for the coefficients a_n by the Schmidt method [6]. It can be seen in [3].

4. Intensity Factors

Although we can determine the entire stress field and the electric displacement from coefficients a_n, it is of importance in fracture mechanics to determine stress τ_{yz} and the electric displacement D_y in the vicinity of the crack's tips. τ_{yz} and D_y along the crack line can be expressed respectively as

$$
\begin{aligned}
\tau_{yz}(x,0) &= \tau_{yz}^{(1)}(x,0) \\
&= -\frac{1}{\pi}\sum_{n=0}^{\infty} a_n Q_n \Bigg[\int_0^\infty c_{44} G_n(s) J_{n+1}\left(s\frac{1-b}{2}\right)\cos(xs)\,\mathrm{d}s \\
&\quad - \frac{\mu}{\pi}\int_0^\infty \frac{\cosh(sx)s}{\sinh(sh)+\mu_1\cosh(sh)}\,\mathrm{d}s \int_0^\infty G_n(\eta) J_{n+1}\left(\eta\frac{1-b}{2}\right) \\
&\quad \times \frac{\eta\sin(\eta h)-s\mu_1\cos(\eta h)}{(\eta^2+s^2)\eta}\,\mathrm{d}\eta \\
&\quad + \frac{e_{15}^2}{\pi\varepsilon_{11}}\int_0^\infty \frac{\cosh(sx)s}{\sinh(sh)}\,\mathrm{d}s \int_0^\infty G_n(\eta) J_{n+1}\left(\eta\frac{1-b}{2}\right)\frac{\sin(\eta h)}{(\eta^2+s^2)}\,\mathrm{d}\eta\Bigg] \qquad (27)
\end{aligned}
$$

$$
\begin{aligned}
D_y(x,0) &= D_y^{(1)}(x,0) \\
&= -\frac{e_{15}}{\pi}\sum_{n=0}^{\infty} a_n Q_n \Bigg[\int_0^\infty G_n(s) J_{n+1}\left(s\frac{1-b}{2}\right)\cos(xs)\,\mathrm{d}s \\
&\quad -\frac{1}{\pi}\int_0^\infty \frac{\cosh(sx)s}{\sinh(sh)}\,\mathrm{d}s \int_0^\infty G_n(\eta) J_{n+1}\left(\eta\frac{1-b}{2}\right)\frac{\sin(\eta h)}{(\eta^2+s^2)}\,\mathrm{d}\eta\Bigg] \qquad (28)
\end{aligned}
$$

Observing the expression in (27) and (28), the singular portion of the stress field and the singular portion of electric displacement can be expressed respectively as following:

$$
\tau = -\frac{c_{44}}{2\pi}\sum_{n=0}^{\infty} a_n Q_n H_n(b,x), \qquad D = -\frac{e_{15}}{2\pi}\sum_{n=0}^{\infty} a_n Q_n H_n(b,x) \qquad (29)
$$

where

$$
H_n(b,x) = \begin{cases} (-)^{n+1} F_1(b,x,n), & n = 0,1,2,3,4,5,\ldots \quad (0 < x < b) \\ -F_1(b,x,n), & n = 0,1,2,3,4,5,\ldots \quad (1 < x) \end{cases}
$$

$$
F_1(b,x,n) = \frac{2(1-b)^{n+1}}{\sqrt{(1+b-2x)^2-(1-b)^2}\,[|1+b-2x| + \sqrt{(1+b-2x)^2-(1-b)^2}]^{n+1}}
$$

At the left tip of the right crack, the stress intensity factor K_{L} can be expressed as

$$
K_{\mathrm{L}} = \lim_{x\to b^-}\sqrt{2\pi(b-x)}\cdot\tau = c_{44}\sqrt{\frac{1}{2\pi(1-b)}}\sum_{n=0}^{\infty}(-1)^n a_n Q_n \qquad (30)
$$

At the right tip of the right crack, the stress intensity factor K_{R} can be expressed as

$$
K_{\mathrm{R}} = \lim_{x\to 1^+}\sqrt{2\pi(x-1)}\cdot\tau = c_{44}\sqrt{\frac{1}{2\pi(1-b)}}\sum_{n=0}^{\infty} a_n Q_n \qquad (31)
$$

At the left tip of the right crack, the electric displacement intensity factor $K_{\mathrm{L}}^{\mathrm{D}}$ can be expressed as

$$
K_{\mathrm{L}}^{\mathrm{D}} = \lim_{x\to b^-}\sqrt{2\pi(b-x)}\cdot D = e_{15}\sqrt{\frac{1}{2\pi(1-b)}}\sum_{n=0}^{\infty}(-1)^n a_n Q_n = \frac{e_{15}}{c_{44}}K_{\mathrm{L}} \qquad (32)
$$

At the right tip of the right crack, the electric displacement intensity factor K_R^D can be expressed as

$$K_R^D = \lim_{x \to 1^+} \sqrt{2\pi(x-1)} \cdot D = e_{15}\sqrt{\frac{1}{2\pi(1-b)}} \sum_{n=0}^{\infty} a_n Q_n = \frac{e_{15}}{c_{44}} K_R \tag{33}$$

5. Numerical Calculations and Discussion

From the work [3], it can be seen that the Schmidt method is performed satisfactorily if the first 10 terms of the infinite series to equation (26) are obtained. The piezoelectric layer is assumed to be the commercially available piezoelectric PZT-4 or PZT-5H, and the half planes are either aluminum or epoxy. The material constants of PZT-4, PZT-5H, aluminum and epoxy can be found in [3]. The results of the present paper are shown in Figures 2–6, respectively. From the results, the following observations are very significant:

(i) The stress intensity factors and the electric displacement intensity factors not only depend on the crack length, the width of the piezoelectric layer, but also depend on the properties of the materials.

(ii) The effects of the two collinear cracks decrease when the distance between the two collinear cracks increases, that is, the stress intensity factors and the electric displacement intensity factors decrease with the length of the crack decrease.

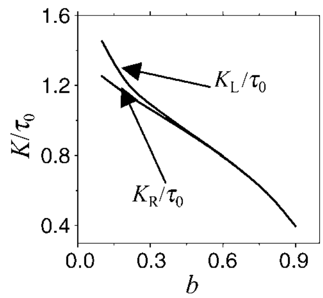

Figure 2. The stress intensity factor versus b for $h = 1.5$ (aluminum/PZT-5H/aluminum).

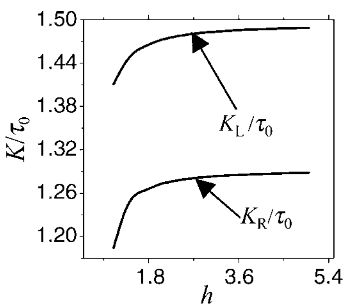

Figure 3. The stress intensity factor versus h for $b = 0.1$ (aluminum/PZT-5H/aluminum).

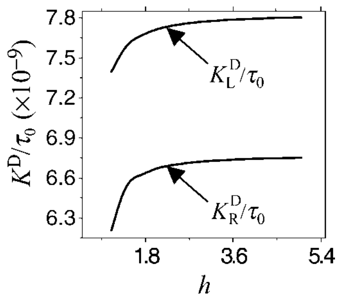

Figure 4. The electric displacement intensity factor versus h for $b = 0.1$ (aluminum/PZT-5H/aluminum).

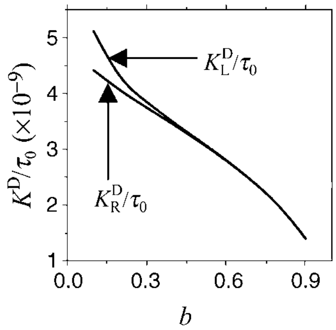

Figure 5. The electric displacement intensity factor versus b for $h = 1.5$ (aluminum/PZT-4/aluminum).

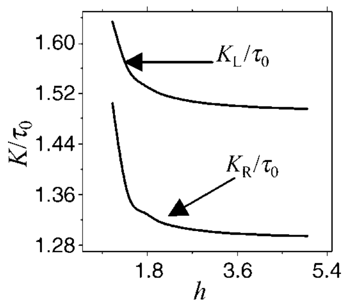

Figure 6. The stress intensity factor versus h for $b = 0.1$ (epoxy/PZT-4/epoxy).

(iii) The stress and the electric displacement intensity factors decrease or increase when the width of the piezoelectric layer increases for the different combination cases of materials, as shown in Figures 3 and 4. So the stress field can reach the minimum value by changing the combination cases of materials.

(iv) The solutions of this paper are approximate to ones of two collinear Griffith cracks in infinite piezoelectric materials for width $h \geqslant 4.0$, that is, the influence of the width of the piezoelectric layer to the results is small for the case $h \geqslant 4.0$, as shown in Figures 3, 4 and 6.

(v) From the results in [3] and the present paper, it can be found that the electric displacement intensity factors for the permeable crack surface conditions are much smaller than the results for the impermeable crack surface conditions. As shown in Figures 4 and 5, the electric displacement intensity factors are very small.

(vi) The stress intensity factors and the electric displacement intensity factors at the inner crack tips are larger than ones at the outer crack tips. However, the stress and electric displacement intensity factors at the inner crack tips are almost equal to ones at the outer crack tips for $b > 0.6$.

Acknowledgements

The authors are grateful for financial supported by the National Natural Science Foundation of China Through the Key Program (50232030) and the National Natural Science Foundation of China (10172030)

References

1. Deeg, W.E.F., *The Analysis of Dislocation, Crack and Inclusion Problems in Piezoelectric Solids*, PhD Thesis, Stanford University, 1980.
2. Pak, Y.E., 'Crack extension force in a piezoelectric material', *J. Appl. Mech.* **57** (1990) 647–653.
3. Zhou, Z.G., Chen, J.Y. and Wang, B., 'Analysis of two collinear cracks in a piezoelectric layer bonded to two half spaces subjected to anti-plane shear', *Meccanica* **35** (2000) 443–456.
4. Zhang, T.Y. and Hack, J.E., 'Mode-III cracks in piezoelectric materials', *J. Appl. Phys.* **71** (1992) 5865–5870.
5. Soh, A.K., Fang, D.N. and Lee, K.L., 'Analysis of a bi-piezoelectric ceramic layer with an interfacial crack subjected to anti-plane shear and in-plane electric loading', *Eur. J. Mech. A/Solids* **19** (2000) 961–977.
6. Morse, P.M. and Feshbach, H., *Methods of Theoretical Physics*, Vol. 1, McGraw-Hill, New York, 1958, pp. 925–937.
7. Gradshteyn, I.S. and Ryzhik, I.M., *Table of Integral, Series and Products*, Academic Press, New York, 1980, pp. 1025–1031.